EUROGRAPHICS '0x / Ken Museth, Torsten Möller, and Anders Ynnerman (Editors)

Volume 0 (1981), Number 0

Integrating Local Feature Detectors in the Interactive Visual Analysis of Flow Simulation Data

Raphael Bürger[2], Philipp Muigg[1], Martin Ilcík[1], Helmut Doleisch[1], and Helwig Hauser[1]

[1]VRVis Research Center, Vienna, Austria
[2]Institute of Computer Graphics , Vienna University of Technology, Austria

Abstract

We present smooth formulations of common vortex detectors that allow a seamless integration into the concept of interactive visual analysis of flow simulation data. We express the originally binary feature detectors as fuzzy-sets that can be combined using the linking and brushing concepts of interactive visual analysis. Both interaction and visualization gain from having multiple detectors concurrently available and from the ability to combine them. An application study on automotive data reveals how these vortex detectors combine and perform in praxis.

1. Introduction

There is still no ultimate agreement on how to generally define and detect vortices, even though the concept of a vortex is common in fluid dynamics and has proven useful to describe and model the behavior of fluids. It is widely agreed that vortices belong to the most important coherent features in flow fields. They influence the behavior of the flow on all scales and are responsible for phenomena like hurricanes and tornadoes, mixing of fluid materials, have influence on the effectiveness of engines and machinery, and the drag on moving objects.

Reportedly local vortex extraction methods fail to find all vortices in real-world data [CBA05]. For example, if there are two axes of swirl, many local detectors will indicate a direction that is a combination of the two [RP98]. The relations between the different criteria have been investigated on a formal basis [CQB99, CPC90, PC87], still the reasons for their different performances are not fully understood. At the moment, there is no answer to the question which detector will perform best in a given situation in general. Especially as long as there is no final answer to the question 'what exactly is a vortex?', we suggest to use a hybrid approach in visual analysis that combines the strengths of more than one criterion.

While most detectors are prone to find false positives [HK99], they do not share exactly the same numerical delicacies. In this paper we discuss how the different vortex extraction schemes can be mapped into a common framework so that the user can analyze how they interact and complement each other for a given problem. This requires to extend the binary classifiers to generate fuzzy response values. To convey the uncertainty that results from vortex feature derivation we use transparency coding and direct volume rendering of the selected regions [DKLP01]. We show how derived features integrate into the process of interactive visual analysis. Until recently the rising computation power has led mainly to rising complexities in the data generated. We propose higher-order features for visual analysis as an end to meet this challenge by incorporating complex automated feature detectors into the process of visual analysis.

SimVis [DGH03] is a relatively new technology designed for the visual inspection of CFD datasets mainly in the context of applied industrial research. It is build on the concepts of smooth attribute selections and the combination of multiple criteria for feature detection. Being able to detect vortices in a reliable and robust manner is of interest since it will allow to inspect the related sub-regions and understand their properties. In the SimVis framework it is useful to have a bouquet of vortex detectors at hand to take advantage of their different behaviors. Accordingly, we have implemented several of the most important local feature detectors and can discuss the results in the context of real-world data. The integration of these feature detectors in our smooth brushing framework of SimVis immediately resulted in very positive response of one of our application partners.

2. State of the art

In this section we briefly recapitulate the SimVis approach to interactive visual analysis, especially also the concept of smooth brushing and linking. Then we give an overview of the most common vortex detectors that serves as a basis for their smooth counterparts, described right afterwards. A more general overview was published by Post et al. [PVH*03].

Interactive extraction of information has been a hot research topic in recent years focusing on interactive information drill-down [Shn96], visual data mining [Kei02] and visual analytics [TC06]. Important issues are advanced interaction concepts and procedures and algorithms to gain access to features and information in the data. The SimVis approach aims at feature-based flow visualization for data exploration and analysis. Advanced interaction mechanisms enable the user to intuitively specify features in the flow data. Multiple, linked views are used to concurrently show different aspects of the flow data. In the visualization, the flow features are visually discriminated from the rest of the data in a focus+context visualization style which is consistent in all views. SimVis supports smooth brushing to enable fractional degree of interest values as well as the logical combination of brushes for the specification of complex features [DGH03]. Brushing means to select intervals of the data values. The data elements that have attribute values inside these intervals, belong to the focus and are highlighted consistently in all views.

From experiments and from literature inspection we have found a series of flow attributes to be useful for understanding the properties of vortices:

- a point $\mathrm{x} \in \mathbb{R}^3$ and an attribute value $a(\mathrm{x})$
- the data set D and data elements in a r-neigborhood of a point $\mathrm{P}_r(\mathrm{x}) = \{\mathrm{y} \in \mathrm{D}, |\mathrm{x}-\mathrm{y}|^2 < r^2\}$
- linear scaling of attribute values $a(\mathrm{x})$ to the interval $[0,1]$ of a subset of data elements $\mathrm{x} \in \mathrm{S} \subseteq \mathrm{D}$ with minimum $\min = \min\{a(\mathrm{x})|\mathrm{x} \in \mathrm{S}\}$ and maximum $\max = \max\{a(\mathrm{x})|\mathrm{x} \in \mathrm{S}\}$ as $scale_{\mathrm{S}}(a(\mathrm{x})) = \frac{a(\mathrm{x})-\min}{\max-\min}$
- the velocity field $\mathbf{v}$
- curl (or vorticity) $\omega = \nabla \times \mathbf{v}$
- the velocity gradient tensor $\mathbf{J} = \nabla\mathbf{v}$ is the Jacobian of $\mathbf{v}$
- the rate-of-strain tensor $\mathbf{S} = \frac{1}{2}(\mathbf{J}+\mathbf{J}^T)$
- the rate-of-rotation tensor $\Omega = \frac{1}{2}(\mathbf{J}-\mathbf{J}^T)$
- there are several criteria working on the parameters of a local curvilinear coordinate system such that $\mathbf{J}$ becomes

$$\nabla\mathbf{v} = [\mathbf{v_r v_{cr} v_{ci}}] \begin{pmatrix} \lambda_r & & \\ & \lambda_{cr} & \lambda_{ci} \\ & -\lambda_{ci} & \lambda_{cr} \end{pmatrix} [\mathbf{v_r v_{cr} v_{ci}}]^{-1}$$

  With $\mathbf{v_r}$, $\mathbf{v_{cr}}$ and $\mathbf{v_{ci}}$ being eigenvectors of $\mathbf{J}$, λ_r the real eigenvalue and $\lambda_{cr} \pm i\lambda_{ci}$ the conjugated complex eigenvalue pair. This differs from the eigenvalues of a symmetric matrix that has three real eigenvalues $\lambda_1 \leq \lambda_2 \leq \lambda_3$.

Levy et al. propose the use of normalized helicity and curl and search for regions where $\mathbf{v}||\omega$ [LDS90]. Even though this may not always correspond to the actual vortex core line, the authors used this feature in combination with color coding successfully on meteorological data.
Hunt's Q criterion compares $\mathbf{S}$ and Ω, with the additional requirement of a local pressure minimum [HWM88].
$\boldsymbol{\lambda_2}$ introduced by Jeong and Hussain [JH95] is one of the most popular vortex detectors and has been studied extensively over the years. The criterion involves computing the symmetric matrix $\mathbf{S}^2+\Omega^2$ and its eigenvalues $\lambda_1 \geq \lambda_2 \geq \lambda_3$. A vortex is the connected region where λ_2 is negative.
Kinematic Vorticity Number N_k is a local measure that gives the quality of rotation independent of vorticity magnitude. It was introduced by Truesdell [Tru54] as $N_k = ||\Omega||/||\mathbf{S}||$. A value of $N_k = \infty$ corresponds to solid body rotation and $N_k = 0$ to irrotational motion.
Chong's criterion is based on critical point theory and the eigenvalues and eigenvectors of the Jacobian. A material particle is considered to show spiralling motion if $\mathbf{J}$ has two complex eigenvectors [CPC90].
Complex eigenvalue related methods can be considered as extensions of the approach of Chong. The swirling strength parameter of Berdahl [BT93] and related methods [ZBA99, CBA05] derive values measuring swirl from the imaginary and real parts of the eigenvalues pair.

3. Contribution

The basic insight that led to the development of the new interactive feature extraction framework is that both automated and interactive approaches have their limits that we can deal with that by combining both approaches. On the one hand, interactive extraction and data analysis is limited in terms of feature complexity. It is simply not possible for the user to find features that have too many dependencies or involve elaborate computations. On the other hand, human users are very good in dealing with incoherent information, uncertainty, and fuzzy concepts. In fact a user will very often know what he was looking for when he has found it [War02]. Automated feature extraction algorithms (in particular vortex detectors) have received intense attention and it is reported that they are all able to detect vortices under the right circumstances in a fast and robust manner.

The detectors currently available may fail to detect non-standard features or features that do not share the same frame of reference as the detector. Furthermore, many feature detection algorithms still need a considerable amount of parameter tuning (e.g. iso-surface values) to get good results. Chakraborty et al. [CBA05], for example, stress the importance of using appropriate thresholds when trying to find vortices with specific properties like compactness along the axis or vortex strength. When multiple features are present there may be no single threshold parameter to detect all flow fea-

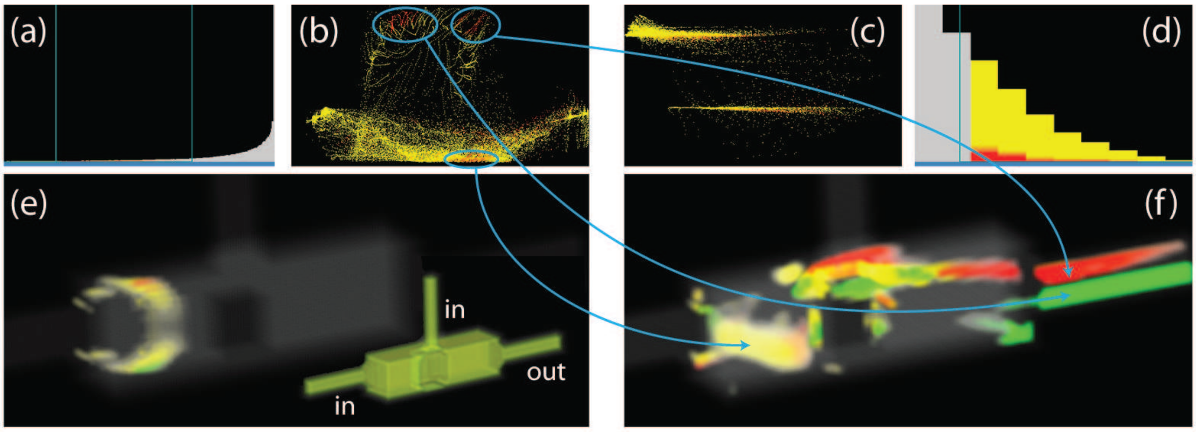

Figure 1: *The combination of smooth feature detectors and interactive visual analysis: (a) The histogram shows that only few data items trigger strong response of the λ_2 feature detector, (b) a scatterplot of temperature against velocity shows differences between the detected vortices, (c) a scatterplot of turbulent energy against relative pressure shows differences between the vortices near the outlet and the inlet (d) a derived distance to surface measure removes occluding elements located at the boundary. (e) This weak vortex in an early time step of the simulation would have broken into several parts using iso-value based visualization; (f) in the 3D overview of the situation we can see how the vortices differ in rotation speed and direction.*

tures at once. Therefore our main motivation to combine visual analysis and algorithmically derived features is to add the monitoring and reasoning capabilities of the user to the exactness and computation power of the computer. See Table 1 for an overview.

3.1. Smooth vortex detectors

To investigate the flow data using focus+context visualization we need to adapt the criteria in a way that they express a notion of "vortexness" as fuzzy-logic attributes. There are some requirements for properties of our fuzzy sets: they should **extend** the binary classifiers (i.e. they are 0 where the binary classifier outputs no vortex and 1 where a vortex would be detected with full certainty). We don't force a measure to be extensive when it is in general also used for other purposes and the user expects different behavior. Otherwise we can often guarantee extensiveness by scaling the output to the $[0,1]$ interval accordingly. We do not expect sharp feature boundaries at the scale of typical flow simulations. It is sensible to expect the classifiers to be **continuous**. To balance these two criteria we model the range of values where the detector only partially detects a vortex. Furthermore, the classifier should be **monotonic**, since this allows for good intuitive combination behavior using the classical fuzzy norms to model the boolean 'and' and 'or' operations using the 'min' and 'max' functions [KMP00].

- We define a fuzzy local extremum around a point x with numerical attribute $a(\mathrm{x})$ with minimum $min = \min\{a(\mathrm{x})|x \in \mathrm{P}_r\}$ and maximum $\max\{a(\mathrm{x})|x \in \mathrm{P}_r\}$ in a neighborhood as

$$extremum_{Fuzzy}(a(\mathrm{x})) = \begin{cases} 0.5 & : \quad max = min \\ scale_{\mathrm{P}_r}(a(\mathrm{x})) & : \quad otherwise \end{cases}$$

This is, the relative position of the attribute value inside the interval of the minimal and maximal attribute values in the neighborhood of x. Of course a local attribute extremum defined like this is dependent on the extent of the neighborhood that defines localness. This attribute was added because in many typical flow situations it is possible to find the central regions of a vortex by restricting the detected region further using the additional condition of locally minimal pressure.

- The straightforward way to look for vortices is to search for regions of high vorticity magnitude. The actual classifier is 'large vorticity' and has reportedly been fairly successful in free shear flows [JH95], but there is no predefined value from which on vorticity is considered large, therefore the SimVis approach allows the user to select which values he or she considers as 'large'.

$$\omega_{Fuzzy} = scale_{\mathrm{D}}(\omega)$$

- Levy et al. [LDS90] introduced normalized helicity H_n. In the limiting case $\mathbf{v}$ is parallel to ω we have $H_n = \pm 1$ and we do not scale this measure since this is the expected behavior

$$H_n(\mathrm{x}) = \frac{\mathbf{v}(\mathrm{x}) \cdot \omega(x)}{|\mathbf{v}(\mathrm{x})||\omega(\mathrm{x})|}$$

- The characteristic equation for $\boldsymbol{J}\mathbf{J}$ is given by

$$\lambda^3 + P\lambda^2 + Q\lambda + R = 0$$

Method	Properties	Benefits in combined application
Vorticity magnitude	fast computation	can be used for preselection of relevant cells in large data sets using a relaxed threshold
N_k	independent of vorticity magnitude	can be used to cross-check regions selected using vorticity magnitude
Normalized helicity	signed, gives direction of rotation	combination with other detectors helps to distinguish between connected regions of counter-rotating vortices
Hunt's Q	no computation of eigenvalues necessary, in many cases equivalent to λ_2	numerically more stable for noisy data, comparison with λ_2 for confidence
λ_2	based on eigenvalues of a symmetric matrix, does not distinguish between connected vortices	very good performance, reliability affirmed in many publications
Eigenvalue related methods	detailed insight into vortex properties, need eigenvalues and eigenvectors of the rotation matrix, may introduce numerical issues, more costly	can restrict detected vortex regions to portions of fast/slow spiraling motion, give information on axial stretching and orbital compactness

Table 1: *Comparison of detector properties.*

where P, Q and R are the three invariants of $\mathbf{J}$, defined as $P = -tr(\mathbf{J})$, $Q = -\frac{1}{2}(P^2 - tr(\mathbf{JJ}))$ and $R = -det(\mathbf{J})$. The invariants map both to topological critical point features and tell about physical properties of the flow (e.g. $P = 0$ holds for incompressible flows). Therefore they give a useful complement to the other views. Since plots of P, Q and R are not traditionally vortex extraction criteria we do not scale or transform them in any way but map them directly to scatterplots.

- Hunt et al. suggest regions of positive Q as vortical regions [HWM88] where the magnitude of the rate-of-rotation tensor Ω exceeds the magnitude of the rate-of-strain tensor $\mathbf{S}$. The larger the difference between Ω and $\mathbf{S}$ the higher the certainty that we have found a vortex:

$$Q_{Fuzzy}(x) = \begin{cases} 0 & : \quad Q(\mathrm{x}) \leq 0 \\ scale_{\mathbf{D}}(||\Omega||^2 - ||\mathbf{S}||^2) & : \quad otherwise \end{cases}$$

- Complex Eigenvalues: Critical point theory [CPC90] tells us that a particle will show rotation motion if $\mathbf{J}$ has two complex eigenvalues. In the related regions vorticity is sufficiently strong to cause the rate-of-strain tensor to be dominated by the rate-of-rotation tensor. This can be tested by checking the characteristic polynomial of $\mathbf{J}$ for a positive discriminant as we know from Cardan's solution for cubic polynomials. Berdahl and Thompson [BT93] used the fact that in a locally curvilinear coordinate system spanned by the eigenvectors of $\mathbf{J}$ the eigenvalues give insight into the behavior of a fluid particle: If the eigenvalues are complex, then one plane will contain a focus and solution trajectories will wrap around the one real eigenvector. In terms of the eigenvalues the criterion of Chong reads as $\lambda_{ci} > 0$. This criterion was reportedly successfully combined with others [CPC90, ZBA99, RP98].

$$Complex1_{Fuzzy}(\mathrm{x}) = scale_{\mathrm{D}}(\lambda_{ci}(\mathrm{x}))$$

A nice property of this criterion is also that λ_{ci} directly measures the strength of radial motion of a fluid element. Chakraborty et al. [CBA05] suggest a combination of $\lambda_{ci} \geq \varepsilon$ and $\kappa \geq \lambda_{cr}/\lambda_{ci} \geq \delta$ where ε, δ and κ are positive thresholds, to include a notion of orbital compactness of the vortex. From this results an extension to the complex eigenvalue criterion:

$$Complex2_{Fuzzy}(x) = \begin{cases} 0 & : \quad \lambda_{ci}(\mathrm{x}) < \varepsilon \\ scale_{\mathrm{D}}(\frac{\lambda_{cr}(\mathrm{x})}{\lambda_{ci}(\mathrm{x})}) & : \quad otherwise \end{cases}$$

We suggest to use the two criteria in combination.

- Jeong and Hussain [JH95] proposed the second eigenvector λ_2 of $\mathbf{S}^2 + \Omega^2$ as a criterion for finding vortex regions. A vortex is found in regions where λ_2 is smaller than zero. We know that λ_2 requires $\mathrm{x} \cdot \Omega^2 \mathrm{x}$ to be greater than $\mathrm{x} \cdot S^2 x$ in one eigenplane of $\mathbf{S}^2 + \Omega^2$. This is only critical if $\lambda_1 > 0$ since we know that in case $\lambda_1 < 0$ these two are balanced in all directions anyhow. When $\lambda_1 > 0$ the modulus of λ_2 gives indication of the balance of $\mathrm{x} \cdot \Omega^2 \mathrm{x}$ and $\mathrm{x} \cdot \mathbf{S}^2 x$ in one eigenplane of $\mathbf{S}^2 + \Omega^2$.

$$\lambda_{2Fuzzy}(\mathrm{x}) = \begin{cases} 0 & : \quad \lambda_2(\mathrm{x}) \geq 0 \\ 1 & : \quad \lambda_1(\mathrm{x}) \leq 0 \\ scale_{\mathrm{D}}(-\lambda_2(\mathrm{x})) & : \quad otherwise \end{cases}$$

3.2. Integration in the interactive framework

The traditional way of integrating feature detectors in flow visualization is to use iso-surfaces to represent the extracted structures. This is not really appropriate in the case of a vortex. The notion of a continuous degree of interest function tries to capture two important properties of features: the first is that flow features are not sharply defined and the second is the uncertainty that is inherent in feature extraction. Very often we cannot be absolutely confident that each data element we selected really is part of the feature we are looking for. This partial inclusion is represented by rendering data elements with opacity values according to the degree of interest they obtained after all brushes and attributes are summed up. The features are visually represented with their inherent fuzzyness and the user is not tempted to assume a sharp distinction between laminar and turbulent flow.

SimVis suggests a layered work flow. The information drill-down conceptually starts on the direct data access level. The user can get an overview of the distribution of attribute values like temperatures, pressures or flow velocities in the simulation data. This allows us to gain an intuition on the situation in a straight-forward manner.

The second level is analyzing relations between different attributes and different sub-volumes of the simulation. This involves using linked scatterplots of different attributes, interactive brushing and linked views. Feature complexity on this level is still limited to choosing intervals of attribute values to be part of the feature. The selection of specific value ranges involves specifying a degree of interest in parts of the data that exhibit the characteristics selected. In fluid dynamics applications it is very often the case that combinations of different attributes are of interest. For example, we will see in the next section that in the design of a cooling jacket very slow or fast portions of the flow are of critical importance when they have extremely high temperature. The linked aspect of the scatterplots allows us to get an intuition for the relations between multiple attributes.

The third level involves the computation of derived features from one or multiple attributes. On this level general properties of the data like correlation between attributes, time-derivatives of attributes, or smoothing operations result in additional synthetic attributes. After derivation, these synthetic attributes behave like the other attributes and can be brushed, mapped to color, and serve as input information for further derivations. In an iterative manner the user can now use the operations of the higher levels of inspection to gain an understanding of these attributes.

The fourth level tackles specialized feature extraction. After the user has gained insight into the features of the flow it is now possible to choose appropriate feature detectors to extract where and when important events in the flow occur. At this point the interactive aspect of feature detection comes into play: since the interaction with the derived fuzzy set is possible in real-time, one can configure the sensitiveness and related thresholds of the detectors interactively. After visual inspection and parameter tuning these features are ready for access in the higher levels of the work flow. They are ready to be inspected in detail to understand their properties using the upper levels of the SimVis work flow. The other way round the extracted features may be useful for exclusion. An engineer looking for properties of the laminar proportions of the flow can extract a measure of 'vortexness' and brush only those parts that possess low membership values for this fuzzy set.

The possibility to combine different features has the benefit of being able to express complicated vortex criteria using simple combinations. The vortex core extraction operator of Sujudi and Haimes [SH95], for example, can be expressed as a combination of the parallel vectors operator [PR99] and the discriminant criterion of Chong [CPC90]. The vortex core extraction algorithm of Miura and Kida [MK97] is a combination of local pressure minima and parallel vectors. Furthermore combining multiple detectors can help to compensate unwanted properties of one detector. The λ_2 method for example does not always distinguish nearby vortices. This can often be compensated for by deriving a helicity attribute to differentiate nearby vortices by means of rotational direction.

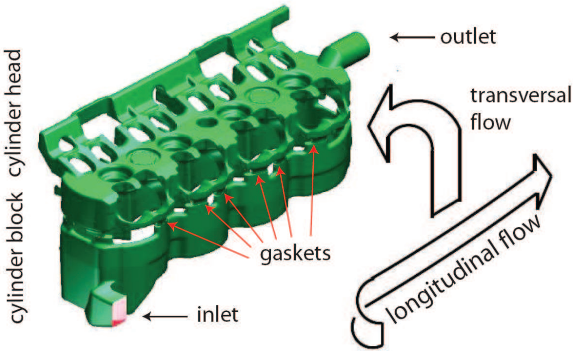

Figure 2: *The major components of the flow through the cooling jacket include a longitudinal component from inlet to outlet and a transversal component in the upward-and-over direction through the gaskets [HLD07].*

In Figure 1 we see an illustration of the discussed qualities: in (a) a histogram of the λ_2 values (high λ_2 to the left and low λ_2 to the right) shows that only a small proportion of cells in the data set exhibit high feature values but a substantial fraction of the data is mapped to non zero vortex membership values. (b) In the scatterplot – mapping temperature against velocity – we can see that the cells belonging to vortices (points highlighted in red) cluster for each vortex. (c) A scatterplot of turbulence against relative pressure shows that there are two main pressure levels and we can interactively check that pressure is lower near the outlet.

The derived feature attributes also add value through the linking functionality – selecting high feature values highlights these data elements in the other views. In part (e) of the image we can see how the mapping to fuzzy values of featureness changes aspects of the visualization: the horseshoe vortex is detected with high fuzzy values in the front part where it is strongest. Near the two ends of the horseshoe it is not very typical and the cells are assigned values close to zero by the detector. In a visualization using iso-value surfaces this vortex would break into several parts due to this effect, but it is conceivable as a whole as a fuzzy-region. This histogram of distance to surface

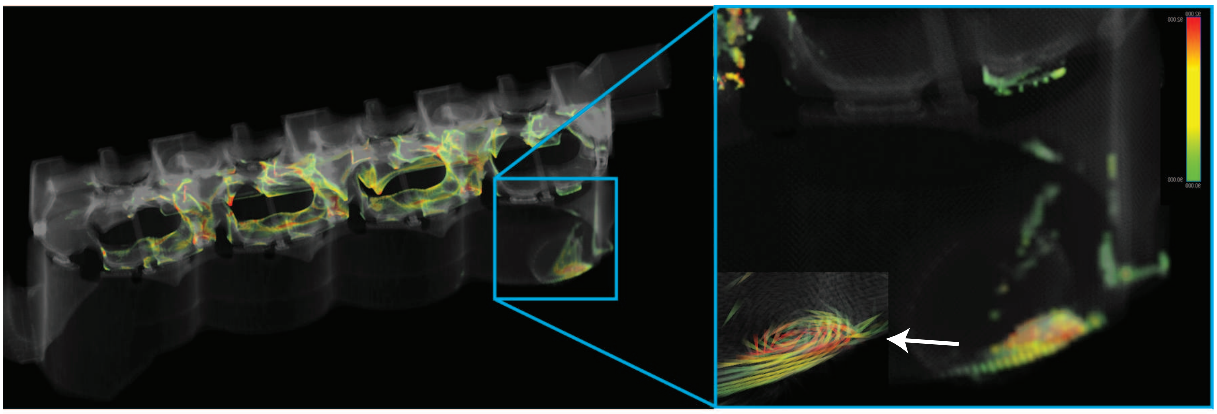

Figure 3: *A feature-based, focus+context visualization showing regions of near stagnant, hot flow with medium to high levels of the λ_2 vortex detector. On the left we see the regions in focus. The zoomed view shows details, especially the extent of critical (red) volume. A refined magnification reveals a vortex structure at this point.*

measure (d) was used to remove obscuring boundary cells from focus. In part (f) we see the features that were found in a 3D view color mapped with helicity to display information on the direction of rotation and its strength.

4. Application Evaluation – a Cooling Jacket

In the following we briefly sketch two examples of interactive visual analysis and exploration of fluid flow through a cooling jacket. Computational fluid dynamics software is used to inspect and improve the design process and we know that engineers invest large amounts of time to optimize the geometry of cooling jackets. In this application evaluation we continue work done by Hauser et al. [HLD07] and Laramee et al. [LH05] where regions of turbulence were not considered. For supplementary documentation and results to this case study, in particular video, high-resolution images and other material, please refer to `www.vrvis.at/via/research/feature-simvis`.

The cooling jacket in focus (see Figure 2) is used with a four cylinder engine. The complex shape of the cooling jacket is influenced by multiple factors including the shape of the engine block and to optimal temperature for the particular engine. The cooling jacket geometry consists mainly of three components: the cylinder head on top, the cylinder block on the bottom and a thin component connecting the cylinder head and block, called the gasket. The cylinder head is responsible for transferring heat away from the intake and exhaust ports at the top of the engine block. The cylinder block is responsible for heat transfer from the engine cylinders and for even distribution of flow to the head. Between the cylinder head and block lies the cooling jacket gasket. It consists of a series of small holes that act as conduits between the block and head. These ducts can be quite small relative to the overall geometry but nonetheless are very important because they are used to govern the motion of fluid flow through the cooling jacket. There are two main components to the flow through a cooling jacket: a longitudinal motion lengthwise along the geometry and a transversal motion from cylinder block to head and form the intake to the exhaust side. Important design goals for the mechanical engineers are to obtain an even distribution of flow to each engine cylinder and to avoid regions of stagnant flow to ensure good overall heat transport.

4.1. Reduced heat transport due to turbulent motion

In order to find regions of the geometry that might need refinement we search for regions where slow flow motion and high temperatures come together. The resulting image is still cluttered from very small regions (that pose no problem to engine operability) and therefore difficult to understand. A similar situation appears in the former investigation of this property in a recent publication by Laramee [LH05]. From background knowledge we know that vortices may diminish heat transport. Figure 3 left illustrates regions in focus after brushing temperatures above the range of optimal conditions around 363° K in combination with a derived vortex measure. The result is a less cluttered image, showing larger undesirable regions, where the cooling fluid is less effective in transporting heat away. There is a large connected region of low heat transport visible in the lower right part of the overview picture. After zooming in and visual inspection of flow behavior we can conclude that the unwanted formation of a vortex is probably the cause for this situation. Fortunately we know from engineers that the region is small enough and operation of the engine in this state remains safe.

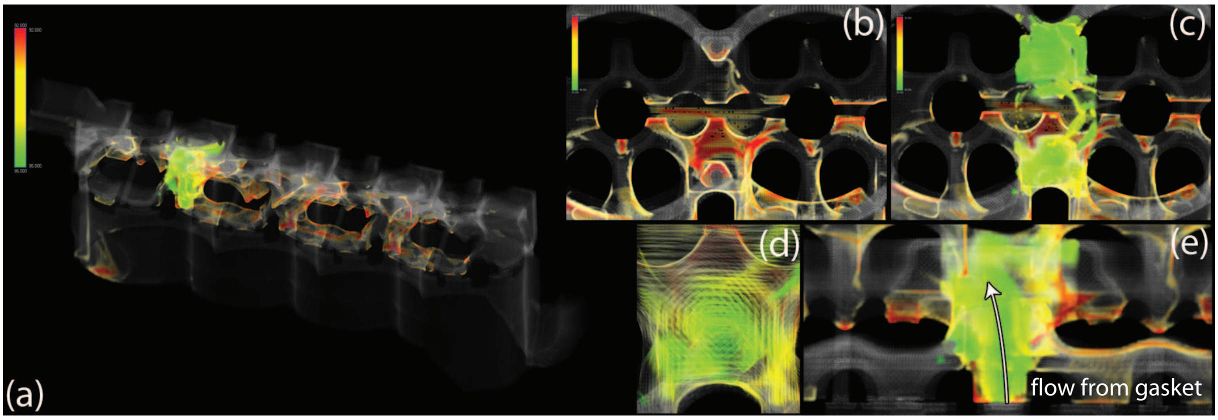

Figure 4: *(a) We have highlighted the turbulent region of interest. (b) From the top we can see that a large patch of the surface contains high temperature values. (c) We additionally include the two regions of turbulence below the surface. The lower one has smaller extent and not enough cooling fluid is transported to this point. (d) A magnified view of the lower turbulent structure. (e) The turbulent structure caused by a gasket, viewed from the side.*

4.2. A situation of improved heat transport due to turbulent motion

Even though the vortex in the preceding paragraph caused problems, there are cases when engineers intentionally induce swirling motion when designing geometry. In Figure 4 we see a region of turbulent motion that was provoked deliberately by choosing an appropriate gasket geometry. Why is this so? The parts of the geometry close to the inner boundary where the engine cylinders are located are critical parts of the volume. Turbulent motion mixes the fluid and transports the hot portions away from the boundary replacing them with cooler elements of the fluid. The large overview part of the image (a) tries to give a feeling for the three dimensional geometry of such a region of high turbulence behind a gasket. The next part of the image (b) shows a zoomed view from above. The two ring shaped parts of the geometry hold a cylinder, and we can see that one side has mapped high temperature values (red) while the other is not in the critical temperature interval. Now we include the regions of turbulence caused by two of the opposing gaskets into the view (c). It becomes clearly visible that the side with good temperature values is well covered by the turbulent motion. On the other side the situation is different: the hot parts are not covered by the turbulent motion and receive not enough cooling fluid. In (d) we see an enlarged view of the vortical motion. Due to fuzzy-attribute mapping one can get a good impression of the relative strength of turbulence. The last part of the image (e) shows another view on the region of turbulence from the side.

Technical considerations

SimVis has to handle data sets with up to 1000 time steps, 20–50 data attributes and up to several million cells in unstructured grids. Therefore it is important to save resources available when calculating derived features. In this respect storing the feature information that was output by the detector in a float channel is a very good solution since the computations have to be done only once. The additional amount of data is comparatively small and the lazy loading capability of the SimVis prototype supports this approach. To achieve fast visualization of the large amount of cells we use graphics hardware accelerated rendering. To further speed up computationally intensive processes, we use the SSE (Streaming SIMD Extensions) instruction set to compute fuzzy logic operations. SimVis runs interactively on a standard PC (AMD Athlon 64 Dual Core 2,2GHz with a NVidia GeForce 6800 graphics card) for up to 10 million data items. To derive gradients on the unstructured grid data we used a plane fitting technique [Mav03].

Summary and future work

We have shown that feature detection algorithms benefit from smooth representations in the context of interactive visual analysis – both with regard to effectiveness and efficiency. We have discussed how the criteria are fitted into the SimVis framework and contribute to the overall usefulness of the system. Additionally, we have applied this new approach successfully to data from the engineering domain. Due to space-limitations it was not possible to go into further detail on how the different detectors and measures are interrelated and contribute to each other. We plan to investigate the interrelationships of the criteria from the viewpoint of visualization in future work. An interesting question to tackle will be how the interactive combination of several criteria can improve the understanding of complicated vortices and other features of turbulent flow. Furthermore there is the question on how to combine non local and topological methods with the local feature detection criteria.

Acknowledgements

The authors thank Ronny Peikert, Markus Trenker, and Meister Eduard Gröller for their helpful input and discussions leading to shared insight on vortex extraction methods. This work has been partly funded both by the FWF PVG project supported by the Austrian Science Fund (FWF) under grant no. P18547, as well as by the "Bridge" funding program of the Austrian Funding Agency (FFG) in the scope of the "MulSimVis" project (Nr. 812106). The cooling jacket CFD simulation dataset is courtesy of AVL List GmbH, Graz, Austria.

References

[BT93] BERDAHL C. H., THOMPSON D. S.: Eduction of swirling structure using the velocity gradient tensor. *AIAA Journal 31(1)* (1993), 97–103.

[CBA05] CHAKRABORTY P., BALACHANDARAND S., ADRIAN R. J.: On the relationships between local vortex identification schemes. *Journal of Fluid Mechanics 535* (2005), 189–214.

[CPC90] CHONG M. S., PERRY A. E., CANTWELL B. J.: A general classification of three-dimensional flow fields. *Physics of Fluids 2* (1990), 765–777.

[CQB99] CUCITORE R., QUADRIO M., BARON A.: On the effectiveness and limitations of local criteria for the identification of a vortex. *European Journal of Mechanics 18* (1999), 261–282.

[DGH03] DOLEISCH H., GASSER M., HAUSER H.: Interactive feature specification for focus+context visualization of complex simulation data. In *VisSym* (2003), pp. 239 – 248.

[DKLP01] DJURCILOV S., KIM K., LERMUSIAUX P. F. J., PANG A.: Volume rendering data with uncertainty information. In *Data Visualization (proceedings of the EG+IEEE VisSym)* (2001), pp. 243–52.

[HK99] HAIMES R., KENWRIGHT D.: On the velocity gradient tensor and fluid feature extraction. In *Proceedings of AIAA 14th Computational Fluid Dynamics Conference* (1999).

[HLD07] HAUSER H., LARAMEE R., DOLEISCH H.: Topology-based versus feature-based flow analysis - challenges and an application. In *Proceedings of TopoInVis* (2007).

[HWM88] HUNT J. C. R., WRAY A. A., MOIN P.: Eddies, stream and convergence zones in turbulent flows. In *2. Proceedings of the 1988 Summer Program* (1988), pp. 193–208.

[JH95] JEONG J., HUSSAIN F.: On the identification of a vortex. *Journal of Fluid Mech. 285* (1995), 69–84.

[Kei02] KEIM D. A.: Information visualization and visual data mining. *IEEE Transactions on Visualization and Computer Graphics 8*, 1 (2002), 1–8.

[KMP00] KLEMENT E. P., MESIAR R., PAP. E.: *Triangular Norms, volume 8 of Trends in Logic*. Kluwer Academic Publishers, 2000.

[LDS90] LEVY Y., DEGANI D., SEGINER A.: Graphical visualization of vortical flows by means of helicity. *AIAA Journal 28* (1990), 1347–1352.

[LH05] LARAMEE R. S., HAUSER H.: Geometric flow visualization techniques for cfd simulation data. In *SCCG '05: Proceedings of the 21st spring conference on Computer graphics* (2005), pp. 221–224.

[Mav03] MAVRIPLIS D. J.: Revisiting the least-squares procedure for gradient reconstruction on unstructured meshes. In *In proceedings of the 16th AIAA Computational Fluid Dynamics Conference* (2003).

[MK97] MIURA H., KIDA S.: Identification of tubular vortices in turbulence. *Journal of the Physical Society of Japan 66* (1997), 1331–1334.

[PC87] PERRY A., CHONG M.: A description of eddying motions and flow patterns using critical point concepts. *Annual Review of Fluid Mechanics 19* (1987), 125–155.

[PR99] PEIKERT R., ROTH M.: The 'parallel vectors' operator: a vector field visualization primitive. In *Proceedings IEEE Visualization '99* (1999), pp. 263–270.

[PVH*03] POST F., VROLIJK B., HAUSER H., LARAMEE R., DOLEISCH H.: The state of the art in flow visualization: Feature extraction and tracking. *Computer Graphics Forum 22(4)*, 2 (2003), 775–792.

[RP98] ROTH M., PEIKERT R.: A higher-order method for finding vortex core lines. In *Proceedings IEEE Visualization '98* (1998), pp. 143–150.

[SH95] SUJUDI D., HAIMES R.: *Identification of Swirling Flow in 3D Vector Fields*. Technical Report AIAA-95-1715, American Institute of Aeronautics and Astronautics, 1995.

[Shn96] SHNEIDERMAN B.: The eyes have it: A task by data type taxonomy for information visualizations. In *VL '96: Proceedings of the 1996 IEEE Symposium on Visual Languages* (1996), p. 336.

[TC06] THOMAS J. J., COOK K. A.: A visual analytics agenda. *IEEE Comput. Graph. Appl. 26*, 1 (2006), 10–13.

[Tru54] TRUESDELL C. A.: *The Kinematics of Vorticity*. Indiana University Science Serie 19, 1954.

[War02] WARD M. O.: A taxonomy of glyph placement strategies for multidimensional data visualization. *Information Visualization 1*, 3/4 (2002), 194–210.

[ZBA99] ZHOU J., BALACHANDAR S., ADRIAN R.: Mechanisms for generating coherent packet of hairpin vortices in near-wall turbulence. *Journal of Fluid Mechanics 387* (1999), 353–396.